Copy of Total Scalp Irradiation Article by Tung et al in IJROBP

Tung S.S., Shiu A.S., Starkschall G., Morrison W.H., and Hogstrom K.R. Dosimetric evaluation of total scalp irradiation using a lateral electron-photon technique. International Journal of Radiation Oncology Biology Physics, 27:153-160, 1993.

Int. J. Radiation Oncology Biol. Phys., Vol. 27, pp. 153–160
Printed in the U.S.A.

0360-3016/93 $6.00 + .00

● *Technical Innovations and Notes*

DOSIMETRIC EVALUATION OF TOTAL SCALP IRRADIATION USING A LATERAL ELECTRON-PHOTON TECHNIQUE

SAMUEL S. TUNG, M.S.,* ALMON S. SHIU, PH.D.,* GEORGE STARKSCHALL, PH.D.,* WILLIAM H. MORRISON, M.D.† AND KENNETH R. HOGSTROM, PH.D.*

The University of Texas M. D. Anderson Cancer Center, 1515 Holcombe Blvd., Houston, TX 77030

Purpose: To evaluate the radiation dosimetry of a new technique for total scalp irradiation.
Methods and Materials: A treatment technique described by Akazawa (1989) has been studied. During each fraction, two electron and two photon fields are treated. While most of the lateral scalp is treated with the electron fields, a rind of scalp close to the midsagittal plane is irradiated by parallel-opposed lateral photon fields. A wax bolus is used to build up skin dose and to protect the brain from electron dose. The dose distribution and dose-volume histograms were evaluated for different field arrangements using a 3-dimensional treatment planning system. After modifying the technique, *in-vivo* thermoluminescent dosimetry were used to evaluate the dose distributions for the first two patients.
Results: To compensate for the lack of dose from the opposed photon field at the junction, the technique was modified using overlapped fields instead of abutting fields. A field overlap of 3 to 4 mm between the electron and photon fields was found optimal. When used with the field junction shift of 1 cm midway through the treatment, this scheme resulted in a dose uniformity of −5% to +15% of the prescribed dose in the region of abutment. Results of the 3-dimensional dose calculation were supported by *in-vivo* thermoluminescent dosimetry on two patients.
Conclusion: On the basis of computer dose calculations and *in-vivo* dosimetry, Akazawa's technique for scalp irradiation can be improved by using a 3 to 4 mm overlap of electron and photon fields. This modified technique is practical and produces clinically acceptable dosimetry.

Total scalp irradiation, Combined electron-photon treatment, 3-dimensional treatment planning, Abutment dosimetry.

INTRODUCTION

Tumors such as cutaneous lymphoma, melanoma, and angiosarcoma may present with widespread involvement of the scalp and forehead. Total scalp irradiation may be necessary to treat these malignancies. The therapeutic goal is to obtain a uniform dose distribution throughout the entire scalp while minimizing irradiation of the underlying brain. This treatment goal is not easily achieved, mainly due to the geometry of the head and the close proximity of the scalp to the brain. The thickness variation of the scalp, particularly in the presence of gross tumor, complicates the problem even more.

Since 1970, low energy electron beams (6–9 MeV) have been the modality of choice for whole scalp irradiation at the University of Texas M. D. Anderson Cancer Center (MDACC). Because of their finite range, electron beams were used to reduce the brain dose. Our technique had been to treat six fields per fraction from different gantry and couch angles (2, 13, 14). These angles were carefully selected to minimize oblique incidence of the electron beams, since lateral scattering of electrons from an obliquely incident beam can create a significant change of dose distribution (1, 5, 8) due to beam angulation and the bone-scalp interface. However, by doing this, the patient had to be moved to a different position for treatment of each field. These fields were individually delineated by lead cutouts on the skin surface and beam-shaping metalloid inserts in the applicator. In addition, a polymethylmethacrylate (PMMA) scatter plate was required as a bolus material to increase surface dose for each field (2, 6).

This paper was presented at the 33rd Annual Meeting of the American Association of Physicists in Medicine, San Francisco, CA, 21–25 July 1991.

* Department of Radiation Physics. †Department of Clinical Radiotherapy.
Reprint requests to: Kenneth R. Hogstrom, Ph.D., Dept. of Radiation Physics, U. T. M. D. Anderson Cancer Center, 1515 Holcombe Blvd., Houston, TX 77030.

Acknowledgement—This work was supported in part by National Cancer Institute grant CA-06294.
Accepted for publication 26 February 1993.

Although a high dose to the scalp and a negligible dose to the brain could be achieved, the problem with this technique was the difficulty of field matching on a hemispherical surface. To obtain a uniform dose distribution, specific guidelines concerning field abutment were developed (2). Additionally, the field junction lines were shifted halfway through the treatment course; thus, 12 stationary electron fields were required in all.

The dosimetry of the MDACC 12-field electron beam technique was recently evaluated and reported by Able *et al.* (2). Measurements made in an anthropomorphic phantom showed that the dose variation could be as great as −10% to +50% near field junctions. Also, this 12-field technique was labor-intensive and time-consuming for all involved. In the clinic, accurate setup of fields was difficult to achieve, and frequently, daily treatment required an hour.

Recently, a new approach used at the University of California at San Francisco (UCSF) was reported by Akazawa (3). Although this technique involves both electron and photon beams, its concept is considerably simpler because only lateral fields are used and the patient remains in one position during the treatment. The purpose of the present study is to evaluate the field abutment schema of the UCSF technique and to recommend modifications that result in improved dose uniformity. The modified abutment schema is verified by both dose calculations and dose measurements. Based on the results of this study, the total scalp treatment at MDACC has been changed to use this technique in lieu of the 12-field electron technique.

METHODS AND MATERIALS

Treatment technique

Our treatment technique is essentially the same as that described by Akazawa (3). Figure 1 illustrates a typical field arrangement for total scalp irradiation; two pairs of lateral electron and photon fields are treated for each fraction. The main portions of the lateral scalp are irradiated by one of the two lateral electron fields. The remainder of the scalp, which is a median sagittal strip and appears as a "rind" from the lateral view, is treated by a pair of parallel-opposed photon fields. Only four custom blocks are required to define the field shape. The shape of the photon fields must be symmetrical from both sides in order to obtain a uniform dose distribution. However, the shape of the opposed electron fields, except along their junctions with the photon fields, may be changed to conform to different regions of interest. The field border between the electron and photon fields is selected so that minimal brain tissue is irradiated by the photon fields, while the skin surfaces covered by the electron fields are kept from being angulated too much away from perpendicular incidence. A treatment central axis, indicated by ⊕ in Figure 1, is shared by all the fields and is located near the center of the curvature of the field junction. To

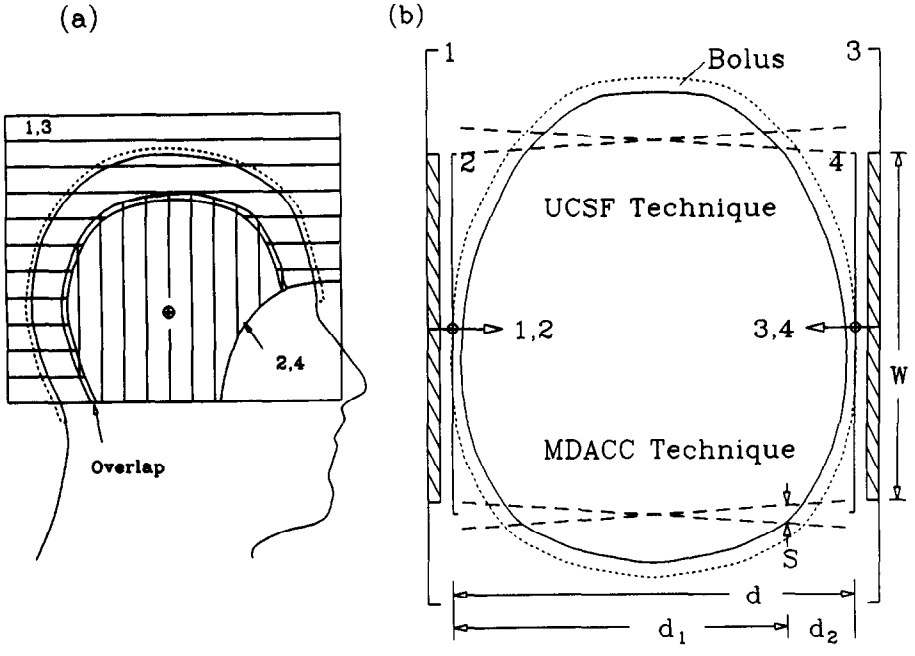

Fig. 1. (a) Lateral view of parallel-opposed field arrangement for the modified UCSF technique. Horizontal lines represent the photon fields 1 and 3, vertical lines the electron fields 2 and 4. ⊕ represents the central axis for both photon and electron fields. (b) Comparison between the UCSF and modified (MDACC) techniques for total scalp irradiation. Dashed lines indicate the edges of photon fields. An electron field overlap is required to boost the dose in the area labeled by "S."

provide dose build-up for photon and electron beams and to spare distal brain tissues from the electron beams, the entire target volume is covered by a bolus of approximately 6 mm thick on the scalp surface.

To improve the dose uniformity, the field junction is shifted during the treatment (3). Since both the patient's set-up and the treatment field center are unchanged, only a new set of field-defining blocks is required for the junction shift. Generally, the first field junction is placed just inside the inner table of the skull (approximately 5 mm) on the lateral simulation film. The junction is shifted toward the field center, making the electron fields smaller.

Rather than exactly abutting the fields as proposed by Akazawa (3), the electron and photon fields are overlapped in our modified technique. A comparison of the UCSF technique and our modifications is illustrated in Figure 1b. This figure contains the central axis and is representative of all planes containing the central axis, since selection of the central axis ensures that the fields abut approximately along an arc of constant radius. Figure 1b illustrates the basis for the modification. As indicated by dashed lines in Figure 1b, the geometric edges of the photon fields are calculated by assuming a 100-cm source-to-surface distance (SSD) to show the field divergence for a typical treatment. Obviously, the beam divergence results in a separation between the two photon field edges on the scalp. The size of the separation on the scalp surface, S, may be derived from the difference in distance between the entrance point of one photon beam and the exit point of the opposed beam ($d_1 - d_2$ in Fig. 1b) by:

$$S = (W/2) \times (d_1 - d_2)/SSD \qquad \text{(Eq. 1A)}$$

$$= (W/2) \times (d - 2d_2)/SSD, \qquad \text{(Eq. 1B)}$$

where W is the width of the blocked field as defined at the SSD, d is the lateral diameter of the head along the central axis, and $d - 2d_2$ is the lateral diameter where the fields overlap. By inserting typical values of W (10 cm) and $d - 2d_2$ (12 cm) into Eq. 1B, the width of the field separation, S, is approximately 6 mm. Geometrically, the scalp tissue in this 6-mm separation area is not exposed to the opposed photon beam and receives radiation only from a single photon field. The remaining treatment areas are irradiated to a uniform dose by either two photon fields or a single electron field. Therefore, to avoid underdosage in the separation regions, it is necessary to overlap the electron and photon fields.

3-Dimensional dose calculation

To compare different field arrangements, a 3-dimensional treatment planning system (11) was used to calculate the dose distributions and dose-volume histograms (DVHs). The DVHs were calculated using a technique that selects at least 500 randomly located points in the volume of interest. For electron dose calculations, the standard pencil-beam model was implemented to calculate the dose distributions on a 3-dimensional grid with 3-dimensional heterogeneity correction (7, 12). For photon dose calculations, the algorithm is based on the scatter-summation method developed by Cunningham *et al.* (4).

To demonstrate the ability of the system, the dose distributions from different beams were first calculated using a water phantom geometry to compare with beam data measured by 0.1 cm^3 air ionization chamber. For the photon and electron beams* used in this study the maximum dose differences between the calculated and measured dose distributions, including the penumbral regions, were less than either 1 mm or 4% at the point of interest.

Dose verification measurements

Thermoluminescent dosimeters (TLDs) were used to measure the dose *in vivo* at selected points on the skin surface of two patients. Measurements were made at the beginning of each treatment course to verify the treatment setup and delivered dose. The TLD packs were selected to be thin (1 mm) in the depth dimension because of the sharp dose gradient of the electron beam in that direction. The cross section (5×5 mm^2) of the TLD packs resulted in an averaged skin surface dose over that area. Each polyethylene TLD pack contained approximately 27 mg of lithium fluoride (TLD-100) powder. They were taped directly to the patient's skin surface under the bolus. For each TLD pack, the TL material was weighed and read approximately 24 hr after irradiation. The dose response of the TLD to both electron and photon beams was calibrated at the depth of dose maximum (d_{max}) in a water phantom for each beam. The difference in sensitivity (dose per thermoluminescent output) between the electron and photon beams was less than 2%. Hence, it was possible to leave the TLD in position throughout the treatment of all four fields and to use the average sensitivity to convert TLD readings into radiation doses.

RESULTS AND DISCUSSION

Field determination

A set of computed tomography (CT) images taken every 5 mm from a patient in typical treatment position was used for 3-dimensional dose calculations. To achieve a uniform dose, the 6-MeV electron and 6 MV photon beams were weighted 100% and 60%, respectively. It should be noted that this weighting scheme is appropriate for the typical lateral diameter of the head of approximately 15 cm; however, significantly smaller (larger) heads may require somewhat lesser (greater) photon beam

* Varian Clinac 2100C, 6 MV X-ray and 6-MeV electron beams; Siemens Mevatron KD, 6 MV X ray and 7-MeV electron beams.

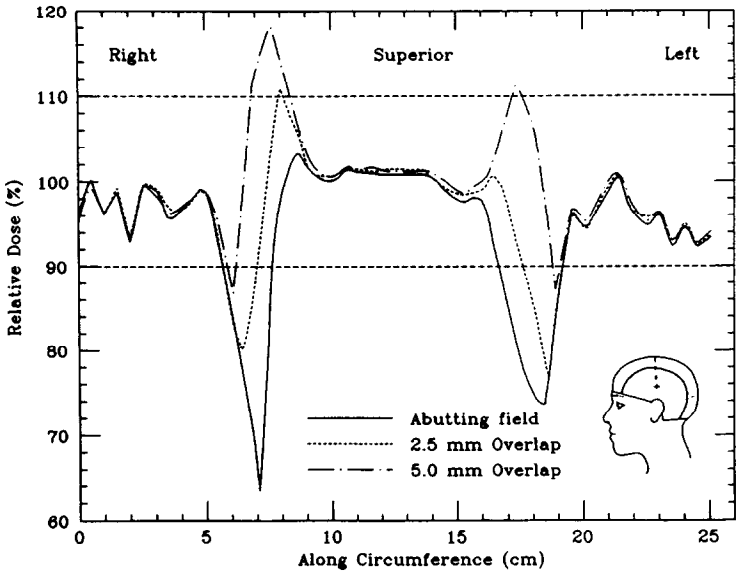

Fig. 2. Comparison of skin surface dose profiles from different field overlaps without junction shift. Dose is normalized to the given dose of one electron field. Profiles are calculated along the head circumference through a coronal plane (insert).

weightings. The beam weights represent the maximum dose delivered to the central-axis from the unblocked (open) field with an SSD equal to the source-to-isocenter distance (100 cm). To determine the optimal field overlap, the dose distributions were first calculated with different field overlaps, namely 5.0 mm, 2.5 mm, and 0 mm (abutting fields). The relative skin surface doses resulting from the different field overlaps are shown in Figure 2. The surface doses, which are normalized to the weight of the electron beam, are plotted along the head's circumference in a coronal plane. The skin surface doses calculated in the electron fields, that is, 0–5 cm and 20–25 cm along circumference in Figure 2, average approximately 96%. We expect a dose of approximately 95%, 88% being the depth dose of the 6-MeV beam beneath the 0.6 cm bolus, 1% being the bremsstrahlung dose from the opposite electron field, and 6% from transmission of photon dose through the blocked fields of the two photon beams. The skin surface doses calculated in the photon irradiated volume, that is, 9–15 cm along circumference, are just above

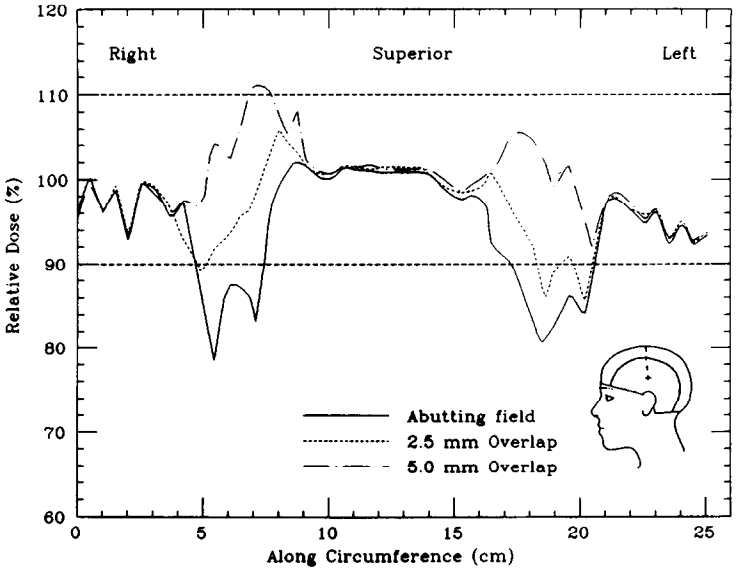

Fig. 3. Comparison of combined skin surface dose profiles from different field overlaps with a 1.0 cm junction shift at 100 cm SSD. Dose is normalized to the given dose of one electron field. Profiles are calculated along the head circumference through a coronal plane (inserts).

100%. The primary purpose of the data is to study the dose distribution in the region of field abutment. If there is no field overlap (solid line in Fig. 2), then the surface doses range from approximately 65% to 103% over the field junctions. Such cold spots will result in a clinically unacceptable dose distribution. To reduce the effect, the amount of overlap between the abutted fields is first increased to 2.5 mm and then 5.0 mm, changing the dose variation to 80% to 110% and 87% to 116%, respectively. As expected, increasing the overlap does not reduce the dose inhomogeneity, but allows the dose variation to be more uniformly spread around the mean dose of the non-abutted region. It appears that the optimal overlap lies between 2.5 and 5.0 mm.

The variation of dose in the region of abutment can be reduced by using a junction shift, at the expense of increasing the size of the region of abutment. Assuming that the shape of the profile is approximately the same before and after the junction shift, the combined dose profile was estimated by translating one of the dose profiles shown in Figure 2 and then summing the two dose profiles together. Using differing magnitudes of junction shifts, several combined dose profiles were generated to compare the ranges of dose variation. It was determined that the optimal shift is about 1.4 cm along the skin surface, which corresponds to a shift of approximately 1 cm perpendicular to the central axis of the treatment field at 100 cm SSD. Figure 3 shows the resulting combined dose profiles. As expected, the junction shift reduces by approximately one half the magnitude of dose variation, while approximately doubling the size of the region of abutment. These results indicate that a field overlap of 3.5 ± 1 mm with a junction shift of 1 cm produces the most uniform dose distribution (100 ± 10%) for this case.

3-Dimensional dose distribution

Based on the above observations, 3-dimensional dose distributions of an eight-beam composite plan were calculated using the following parameters:

- Beam energies: 6 MV X-rays and 6 MeV ($E_{p,0}$ = 6.3 MeV) electrons;
- Field overlap: 4 mm;
- Junction shift: 1.0 cm at 100 cm SSD;
- Equal weighting before and after junction shift.

For this example, a dose of 55 Gy was originally prescribed to the 90% isodose contour. Thus, each of the four electron fields were weighted 30.6 Gy, and each of the four photon fields were weighted 18.3 Gy (60% of 30.6 Gy). Figure 4 shows the resulting dose distributions in two principal anatomical planes: a transverse CT plane close to the central axis (Fig. 4a) and the midsagittal plane (Fig. 4b) with structure contours reconstructed from structures individually outlined on the set of transverse CT images spaced every 5 mm. Results show that the dose to most of the brain is relatively low because the primary contribution

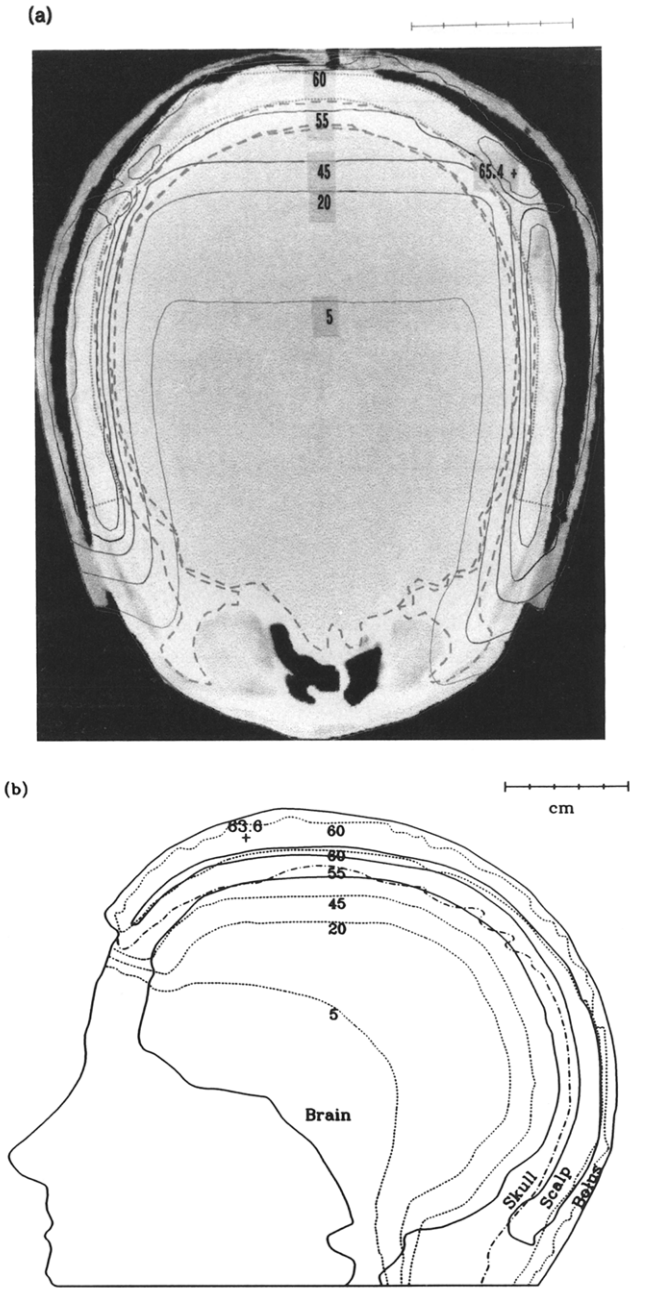

Fig. 4. Composite dose distributions for a sarcoma patient with a prescribed dose of 55 Gy. (a) transverse and (b) midsagittal planes from 3-dimensional dose calculations. Isodose contours shown are 60, 55, 45, 20, and 5 Gy with location of maximum dose indicated by "+."

is the transmitted radiation through the field-defining blocks of the photon fields. A small region of the brain, which is near the midsagittal plane and brain-skull interface, is exposed to doses higher than 45 Gy because that volume is included in the photon fields. This 45 Gy isodose contour approximately follows the brain-skull boundary, as shown in Figure 4b. Hence, the volume of the brain tissue irradiated by a certain isodose line depends on the location of the intersection of the photon fields. In this case, the photon fields intersected 0.5 cm inside the

brain-skull interface before the 1-cm field shifts, and as shown in Figure 4b, the thickness of 45 Gy line is less than 1 cm inside the brain.

In Figure 4a, the scalp is well covered by the prescribed dose (55 Gy) except for a very small region close to the right skull-scalp interface. This region is in the field junction and would receive a lower dose of 45 Gy. This is primarily due to the increased scalp thickness, which places the scalp-skull interface slightly beyond the therapeutic range (R_{90}) of the 6-MeV beam. To appreciate quantitatively the dose distribution in 3-dimensions, the DVHs of the scalp and brain are plotted with solid lines in Figure 5. From a clinical point of view, a higher electron energy would assure better coverage through regions where the treatment target might be thicker due to tumor nodules, surgical reconstructures, or irregularities of bolus thickness. Thus, the physician selected a 7-MeV electron beam ($E_{p,0}$ = 7.4 MeV) for this patient's treatment. For comparison, Figure 5 also shows the DVHs for the 7-MeV electron beam treatment. As expected, when using the higher energy electron beam, the tumor coverage is somewhat better but the dose to brain is slightly higher. Overall, the DVH illustrates that more than 95% of the scalp volume receives a dose greater than 52 Gy (about −5% of prescribed dose), and less than 3% receives a dose greater than 64 Gy (about +15%). Even though photon beams are used in this technique, only about 30% of the whole brain receives more than 10 Gy and 90% of the brain receives less than 45 Gy (see insert in Fig. 5). This dose to the volume of brain irradiated would not be expected to lead to a significant risk of brain injury (9, 10).

In-vivo dose verification

For the first two patients treated using this modified UCSF technique, *in-vivo* dosimetry verification was performed. Daily dose fractions of 200 cGy to the 90% isodose contour were prescribed for both patients. One patient received 30 Gy for the treatment of lymphoma metastases. The other patient, who had a primary dermatofibrosarcoma protuberans, received postoperative irradiation of 50 Gy with an additional boost of 10 Gy using appositional electron fields to the areas where the nodules were excised. The CT study of this sarcoma patient was used for the dose plan described earlier. As shown in Figures 4a and 4b, due to multiple surgical scars and skin graft on this patient's scalp coupled with the bolus fabrication process, there were air gaps as large as 1 cm between the bolus and skin surface. Although one should minimize the air gap for good electron therapy, the nature and magnitude of these gaps are not expected to significantly affect the dose distribution based on our knowledge of the effects of internal inhomogeneities (8). The field overlaps were 3 mm and 4 mm for the lymphoma and sarcoma patients, respectively. The electron beam energies were 6 MeV and 7 MeV, respectively. Thermoluminescent dosimeters packs were placed on the skin surface at selected locations to assess the *in-vivo* dose distributions of a single fraction. Table 1 shows the locations and results of the measurements in which the TLD doses are normalized to the daily given dose of the electron beams (222 cGy). The standard error for the dose measurement is approximately 3%, including the 1% uncertainty due to the difference in the TLD sensitivity between the photon and electron beams.

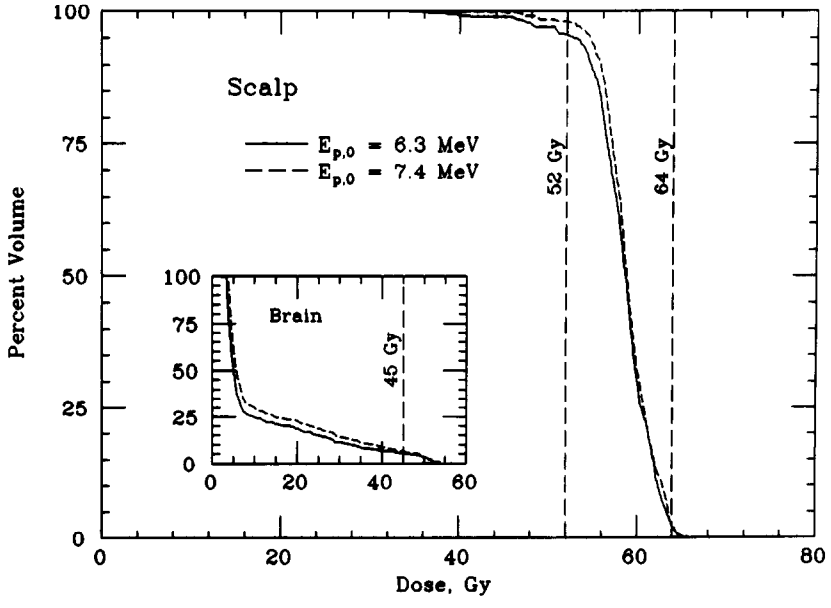

Fig. 5. Dose-volume histogram of scalp and brain (insert) for the same plan shown in Fig. 4. $E_{p,0}$ is the most probable incident energy of the electron beam. Also plotted are the DVHs for $E_{p,0}$ = 7.4 MeV. The dashed lines in the scalp DVH's represent +15% and −5% of prescribed dose.

Table 1. Results of daily TLD measurements on two patients using a modified lateral electron-photon technique

Patient	Percent dose range* (No. of points)			
	R. Lateral	L. Lateral	Midsagittal	All
Sarcoma†	95–97(4)	95–107(5)	94–104(4)	94–107(13)
Lymphoma	95–103(3)	96–100(3)	103 (1)	95–103 (7)

* Doses normalized to 222 cGy.

† TLD location see insert at right.

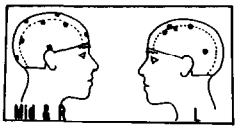

Uniform dose coverage to the entire scalp surface is provided for both patients with the dose having a range from 94% to 107% for the sarcoma patient and 95% to 103% for the lymphoma patient. These results are within the range of skin surface doses from 86% to 116% expected from Figure 2. The measured dose spread is considerably less, in part because the doses were averaged over the physical size (5×5 mm^2) of the TLD.

CONCLUSION

To improve the dose distribution, the UCSF treatment technique using lateral electron-photon fields for total scalp irradiation has been modified. The critical factor for uniformity of dose to the scalp is the schema for field overlap at the field abutment. If the edges of the electron and photon fields are abutted, then an underdose to the scalp appears inevitable in the vicinity of the junction. This underdose is mainly a result of the photon beam's divergence from the edge of the central block of the opposite field. To obtain a more uniform dose distribution in the junction region, our results show that the electron field should overlap the photon field by approximately 3–4 mm. The optimal field overlap may depend on other factors, such as the shape of the electron and photon fields' penumbras, the slope and thickness of the scalp, and the thickness and shape of the bolus. Therefore, computerized 3-dimensional treatment planning is beneficial for each patient. The field arrangement we described should be used only as a starting point for the treatment planning dose calculation, and minor adjustments should be made as needed. In addition, 3-dimensional dose calculation is useful to show whether there is any significant overdose to the brain.

To alleviate the problem of matching fields and to obtain clinically acceptable dose uniformity, the junction shift is necessary. However, the optimal junction shift may be compromised in order to avoid delivering a high dose to the brain. As a reasonably homogeneous dose is obtained by using appropriate field overlap, the amount of the junction shift can be decreased to reduce the brain dose. The brain dose is determined by two main factors: (a) the energy of the electron beam and (b) the location of the photon field. To minimize the dose to the brain, the electron fields should be as large as possible and the electron energy should be the lowest which provides adequate tumor coverage.

Thermoluminescent dosimeters measurements were also made to verify dose delivered by this technique, especially near the field junctions. The *in-vivo* dose measurements demonstrated good dose coverage to the entire scalp surface. Although TLD's measured the doses averaged over a small volume defined by their physical size, the measurements supported and agreed with the 3-dimensional dose calculations.

A linear accelerator that produces both low-energy electron and photon beams is suitable to deliver the total scalp treatment. The patient should generally be treated in a prone position with an appropriate immobilization device, such as a face-mask type head holder. A custom, 6 mm thick wax bolus should be made before treatment to provide buildup as well as sidescatter for good surface dose coverage. The bolus also protects the brain from the electron dose. Only four fields defined by standard beam-shaping blocks are required for each treatment fraction. A 3-dimensional treatment plan is valuable in selection of electron energy and verification of the dose distribution. Our clinical experience demonstrates that patient setup is easy, taking about 20 min for each treatment. In summary, this modified UCSF treatment technique is a relatively simple and reproducible technique, and it provides a better dose distribution than the previously used MDACC 12-field electron technique, while the potential risk to the brain is still very low. Furthermore, total scalp irradiation using this technique should be possible in most radiotherapy centers which have appropriate electron beam capabilities and treatment planning tools.

REFERENCES

1. AAPM, American Association of Physicists in Medicine Task Group No. 25. Clinical electron-beam dosimetry. Med. Phys. 18:73–109;1991.
2. Able, C. M.; Mills, M. D.; McNeese, M. D.; Hogstrom, K. R. Evaluation of a total scalp electron irradiation technique. Int. J. Radiat. Oncol. Biol. Phys. 21:1063–1072;1991.
3. Akazawa, C. Treatment of the scalp using photon and electron beams. Med. Dosim. 14:129–131;1989.
4. Cunningham, J. R.; Shrivastava, P. N.; Wilkinson, J. M. Program IRREG-Calculation of dose from irregularly shaped radiation beams. Comput. Progr. Biomed. 2:192–199;1972.

5. Ekstrand, K. E.; Dixon, R. L. The problem of obliquely incident beams in electron-beam treatment planning. Med. Phys. 9:276–278;1982.
6. Hogstrom, K. R. Treatment planning in electron beam therapy. In: Vaeth, J. M., Meyer, J. L., eds. Frontiers in Radiation Therapy and Oncology, Vol. 25, The role of high energy electrons in the treatment of cancer. Basel, Switzerland: S. Karger; 1991:30–52.
7. Hogstrom, K. R.; Mills, M. D.; Almond, P. R. Electron beam dose calculations. Phys. Med. Biol. 26:445–459;1981.
8. Hogstrom, K. R. Dosimetry of electron heterogeneities. In: Wright, A., Boyer, A. L., eds. AAPM Medical Physics Monograph No. 9: Advances in radiation therapy treatment planning. New York: American Institute of Physics; 1982: 223–243.
9. Marks, J. E.; Baglan, R. J.; Prassad, S. C.; Blank, W. F. Cerebral radionecrosis: incidence and risk in relation to dose, time, fractionation and volume. Int. J. Radiat. Oncol. Biol. Phys. 7:243–252;1981.
10. Sheline, G. E.; Wara, W. M.; Smith, V. Therapeutic irradiation and brain injury. Int. J. Radiat. Oncol. Biol. Phys. 6:1215–1228;1980.
11. Starkschall, G.; Bujnowski, S. W.; Wang, L. L.; Shiu, A. S.; Boyer, A. L.; Desobry, G. E.; Wells, N. H.; Baker, W. L.; Hogstrom, K. R. A full three-dimensional radiotherapy treatment planning system. Med. Phys. 18:647(abst);1991.
12. Starkschall, G.; Shiu, A. S.; Bujnowski, S. W.; Wang, L. L.; Low, D. A.; Hogstrom, K. R. Effect of dimensionality of heterogeneity corrections on the implementation of a three-dimensional electron pencil-beam algorithm. Phys. Med. Biol. 36:207–227;1991.
13. Tapley, N. V. Electron beam. In: Fletcher, G. H., ed. Textbook of radiotherapy, 3rd edition. Philadelphia, PA: Lea & Febiger; 1980:40–60.
14. Tapley, N. V. Skin and lips. In: Tapley, N. D., ed. Clinical application of the electron beam. New York: Wiley & Sons Inc.; 1976:93–123.